Simulations of Vapor–Liquid Phase Equilibrium and Interfacial Tension in the CO_2–H_2O–NaCl System

Yang Liu, Thomas Lafitte, Athanassios Z. Panagiotopoulos, and Pablo G. Debenedetti
Dept. of Chemical and Biological Engineering, Princeton University, Princeton, NJ 08544

DOI 10.1002/aic.14042
Published online March 1, 2013 in Wiley Online Library (wileyonlinelibrary.com)

Direct interfacial molecular dynamics simulations are used to obtain the phase behavior and interfacial tension of CO_2–H_2O–NaCl mixtures over a broad temperature and pressure range ($50°C \leq T \leq 250°C$, $0 \leq P \leq 600$ bar) and NaCl concentrations (1–4 mol/kg H_2O). The predictive ability of several existing water (SPC and TIP4P2005), carbon dioxide (EPM2 and TraPPE), and sodium chloride (SD and DRVH) models is studied and compared, using conventional Lorentz–Berthelot combining rules for the unlike-pair parameters. Under conditions of moderate NaCl molality (~1 mol/kg H_2O), the predictions of the CO_2 solubility in the water-rich and CO_2-rich phase resemble those in the CO_2–H_2O system [Liu et al., J Phys Chem B. 2011;115:6629–6635]. Consistent with our previous work, the TraPPE/TIP4P2005 model combination gives the best overall performance in predicting coexistence composition and pressure in the water-rich phase. Critical assessments are also made on the ranges of temperature and pressure where particular model combinations work better. The dependence of the interfacial tension on temperature and pressure is better predicted by the TraPPE/TIP4P2005 and EPM2/SPC models, whereas the EPM2/TIP4P2005 model overestimates this property by 10–20%, possibly due to the inadequacy of the combining rules. It is also found that the interfacial tension increases with salt concentration, consistent with experimental observations. © 2013 American Institute of Chemical Engineers
AIChE J, 59: 3514-3522, 2013

Keywords: molecular dynamics simulation, carbon dioxide, water, sodium chloride, solubility, interfacial tension, phase equilibrium, atomistic models, CO_2 sequestration

Introduction

Emissions of long-lived greenhouse gases are believed to be a major driver of climate change.[1] Carbon dioxide (CO_2) is the most important greenhouse gas, accounting for 56.6% of the total annual greenhouse gas emissions in 2004.[1] Prominent among the strategies to lower CO_2 emissions currently under investigation is carbon sequestration,[2] which involves capturing CO_2 and storing it in geological repositories, such as deep saline aquifers, coal beds, and hydrocarbon reservoirs. In these geological reservoirs, sodium chloride (NaCl) is the most common dissolved salt.[3] Therefore, to assess the feasibility of carbon sequestration, it is important to understand the phase behavior of the CO_2–H_2O–NaCl system over a wide range of temperatures and pressures. Interfacial tension is another property of great importance to CO_2 storage, because it governs flow processes and controls the capillary-sealing efficiency.[4,5] Moreover, knowledge of the fluid phase behavior and interfacial properties of the CO_2–H_2O–NaCl system is also necessary in CO_2-based enhanced oil recovery operations[6] and in the design of separation equipment.[7]

Experimental measurements of the solubility of CO_2 in pure water and in aqueous NaCl solutions are difficult and expensive to carry out, and, thus, are only available for a limited number of temperature/pressure/composition conditions (see Refs. 8–10 for a comprehensive review). Many thermodynamic models have shown satisfactory modeling ability at relatively low temperatures and pressures,[6,8,9,11–13] yet they have limited predictive ability at other conditions, for example, high temperatures and pressures near the critical locus.[6,9,14,15] In addition, classical thermodynamic models do not provide insights into the microscopic basis for the thermophysical behavior of fluids. Computer simulations, on the other hand, can bridge the gap between macroscopic properties and microscopic intermolecular interactions. In recent years, computer simulation has become an increasingly attractive tool for fluid property predictions, thanks to the development of sophisticated simulation techniques. Many atomistic models have been developed for the intermolecular interactions of various substances, and the equilibrium properties of pure substances and their mixtures can be determined from Monte Carlo or molecular dynamics (MD) simulations coupled with advanced techniques such as Gibbs ensemble Monte Carlo,[16–18] histogram-reweighting grand canonical Monte Carlo,[19–21] NPT + test particle method,[22] and direct simulations of liquid–vapor interfaces.[23] Advances in computational power are also significant. The utilization of parallel computing, such as open MPI and graphics processing units, has made computer simulations much easier and faster than ever before.[24]

Additional Supporting Information may be found in the online version of this article.

Correspondence concerning this article should be addressed to P. G. Debenedetti at pdebene@princeton.edu.

Somewhat surprisingly, there have been relatively few prior simulation studies of the CO_2–H_2O and CO_2–H_2O–NaCl systems. Vorholz et al.[25] applied Gibbs ensemble simulations to study the phase behavior of the CO_2–H_2O system over the temperature and pressure ranges 75–120°C and 0–200 bar, respectively, and that of the CO_2–H_2O–NaCl system over the temperature and pressure range 100–160°C and 0–100 bar, respectively.[26] Recently, some of us applied histogram-reweighting grand canonical Monte Carlo simulations to study the phase behavior of the CO_2–H_2O system over a broader temperature and pressure range ($50°C \leq T \leq 350°C$ and $0 \leq P \leq 1000$ bar).[27] Histogram-reweighting techniques provide a more accurate route to calculate the phase coexistence properties near critical points but are not suitable for the study of solutions with added salt, due to the extremely low acceptance ratio of adding or deleting strongly interacting electrolytes. Alternatively, the phase equilibrium of the CO_2–H_2O–NaCl system can be obtained using Gibbs ensemble simulations or direct interfacial simulations. In recent years, direct interfacial simulation techniques have become a robust and simple tool to obtain phase equilibrium properties of both pure fluids [28–30] and mixtures,[31–35] primarily because computational capabilities are now adequate for simulating relatively large systems over the appreciable times needed to reach equilibration through diffusion. MD simulations can be efficiently parallelized, allowing significant reduction of computer time compared to serial executions when large systems are considered. MD is an efficient technique for the simulation of dense phases and can be readily applied to increasingly complex systems thanks to the availability of highly optimized open-source packages such as LAMMPS.[36] In addition, this method provides information on the surface tension between coexisting phases.[37–39]

In this work, we study the mutual solubility and interfacial tension in the CO_2–H_2O–NaCl system over a broad range of temperatures (from 50 to 250°C), pressures (from 0 to 600 bar), and NaCl concentrations (1–4 mol/kg H_2O), using direct interfacial MD simulations. We also assess the predictive abilities of several combinations of existing H_2O, CO_2, and NaCl models. To describe water, we use the SPC[40] and TIP4P2005[41] intermolecular potential models. For CO_2, we adopt the EPM2[42] and TraPPE[43] models. The SPC model is chosen because it gives better prediction of water's vapor pressure than most of the water models,[27] which is shown to be a key factor for the predictions of the vapor–liquid equilibrium of the CO_2–H_2O mixture.[27] The TraPPE/TIP4P2005 combination is also the best model to predict the solubility of CO_2 in water at various pressures[27] and is therefore chosen for further investigation. Two models are tested for NaCl: the one developed by Smith and Dang (SD model)[44] and the one recently developed by Deublein et al.[45] (in the following referred to as the DRVH model). The DRVH model was originally developed to reproduce the experimental self-diffusion coefficient of Na^+ and Cl^- and the osmotic coefficient of water in aqueous solutions of alkali halide salts. This model uses a Lennard-Jones potential and, hence, is straightforward to combine with other models adopted in this work. The characteristic energy parameter of this model is significantly larger than that of the SD model.

This article is structured as follows. "Method" section provides methodological details on the interaction potential models used and the simulation approach. "Results and Discussion" section presents the results and comparisons to experimental data. "Conclusions" section lists the main conclusions from this work.

Methods

Model system

All the water models investigated in this study include a Lennard-Jones potential to describe central oxygen–oxygen repulsion and dispersion interactions, and fixed-point charges to represent electrostatic contributions. The SPC water model[40] has three charged sites, corresponding to the three atoms of the water molecule with an HOH angle of 109.47°. In the TIP4P2005 water model,[41] the charge on the oxygen site is moved a short distance toward the hydrogen atoms to a so-called "M-site," and the HOH angle takes the observed value, 104.52°. In the EPM2[42] and TRAPPE[43] CO_2 models, both the carbon and the oxygen atoms are represented by partially charged Lennard-Jones sites. The sodium chloride ions are represented as charged Lennard-Jones particles in both the SD[44] and the DRVH[45] models. The total interaction between two molecules i and j with m and n interaction sites, respectively, is calculated as the sum of Lennard-Jones and Coulomb interactions

$$u_{ij} = \sum_{a=1}^{m} \sum_{b=1}^{n} \left(\frac{q_i^a q_j^b}{4\pi\varepsilon_0 r_{ij}^{ab}} + 4\varepsilon_{ij}^{ab} \left[\left(\frac{\sigma_{ij}^{ab}}{r_{ij}^{ab}} \right)^{12} - \left(\frac{\sigma_{ij}^{ab}}{r_{ij}^{ab}} \right)^{6} \right] \right) \quad (1)$$

where ε_0 is the vacuum permittivity; r_{ij}^{ab} is the distance between sites a and b of molecules i and j; q_i^a is the charge on site a of molecule i; and $\varepsilon_{ij}^{ab}$and σ_{ij}^{ab} are the Lennard-Jones interaction parameters between sites a and b. The intermolecular potential parameters for the models studied in this work are listed in Table 1, Supporting Information.

The commonly used Lorentz–Berthelot combining rules are applied to the interactions between unlike Lennard-Jones sites with the exception of the EPM2 model. In the EPM2 potential, the characteristic distance σ_{ij}^{ab} between unlike sites of carbon dioxide molecules is calculated using the geometric mean rather than the arithmetic mean, as suggested in the original reference.[42] To summarize, the cross-interaction parameters are expressed as

$$\sigma_{ij}^{ab} = \begin{cases} \sqrt{\sigma_i^a \sigma_j^b} & for\ a,b = C_{CO_2}, O_{CO_2}\ for\ the\ EPM2\ model \\ \frac{1}{2}\left(\sigma_i^a + \sigma_j^b\right) & otherwise \end{cases} \quad (2)$$

$$\varepsilon_{ij}^{ab} = \sqrt{\varepsilon_i^a \varepsilon_j^b} \quad (3)$$

Computational methods

MD simulations are used to compute the vapor–liquid interface of the CO_2–H_2O–NaCl system, and all simulations are performed using the LAMMPS package.[36] We follow the standard technique for direct interface computation using canonical conditions whereby a fixed number of molecules are placed in a rectangular box with fixed dimensions $L_x \times L_y \times L_z$ chosen appropriately, so that the thermodynamic state lies inside the two-phase region. If the dimensions of the box are chosen such that $L_x = L_y < L_z$, the system will spontaneously separate into two thermodynamically stable phases separated by a planar interface with its surface located normal to the longer axis.

Although this technique is rather straightforward to apply, the precise selection of the global composition and total

volume V of the system to simulate turns out to be subtle and deserves some additional comments. First, it should be noted that, for a given force-field, number of molecules, and temperature T, we do not know in advance which total volume V will place the system in the pressure region of interest. Second, it is important that the global composition of the simulated system lead to the formation of two equilibrated phases with comparable volumes. Therefore, to determine good values for the input parameters of our simulations, it is necessary to obtain preliminary estimates of the equilibrium mole fractions and specific volumes of each phase. Good approximations for these quantities can, in principle, be extracted from analytical equations of state, although some discrepancies are expected, because analytical theories are generally based on simpler descriptions of the molecular interactions. A different approach is used in this work, consisting of performing short Gibbs ensemble Monte Carlo simulations for a few selected models to extract approximate values of the specific volume of each phase for a set of pressure and temperature conditions of interest. Next, with the additional knowledge of experimental mutual solubility of CO_2 in binary CO_2–H_2O mixtures, we are able to determine appropriate system sizes (total number for each species) for each temperature studied, as well as reasonable starting values for the total volume of the box that would drive the system to phase separate. Once the first equilibrium state point is obtained (at a given temperature), different pressure conditions are obtained by gradually increasing or decreasing the volume of the box.

There is no unique way to determine the initial configuration of the system in this direct interface simulation. One could potentially start from a fully mixed state and wait for the system to evolve and ultimately phase separate, if appropriate conditions are selected. However, to reach equilibrium within reasonable computer time, we prefer to start from initially demixed systems. This is done by first equilibrating two separate simulation boxes, containing the CO_2-rich phase on one side and the water-rich phase (including the salt) on the other. As stated previously that each box's dimensions are chosen carefully so as to correspond to the specific volumes of each phase obtained by preliminary Gibbs ensemble calculations. Following this pre-equilibration step, the two phases are then put into contact by forming a single simulation box.

In this study, the system size varies between 1320 and 3200 particles, including 17–100 Na^+ and Cl^- ions, and 300–600 carbon dioxide molecules. The particle–particle–particle mesh Ewald method[46] with conducting boundary conditions is applied to calculate the long-ranged contributions to the electrostatic energy and forces between particles, with a grid size selected to obtain a relative accuracy of the electrostatic energy of less than one part in 10^4. We use a cutoff of 15 Å for both the Lennard-Jones potential and the real space components of the Ewald summations. In our simulations, we use adequately large system sizes and fairly large cutoffs for pair potentials. We checked that these parameters do not affect the calculated phase equilibrium data and interfacial properties by performing test simulations at half the system size, using smaller cutoffs (12 Å instead of 15 Å); these test simulations gave results statistically identical to the calculations reported here. Both water and CO_2 are treated as rigid bodies and their time evolution is computed using a Nosé–Hoover thermostat[47,48] for the translational and rotational degrees of freedom of the molecules. The velocities and positions of the ions are updated with a constant *NVE* scheme. Note that the mixtures studied contain only a small amount of ions compared to the total amount of CO_2 and water molecules in the simulation box. Consequently, the kinetic energy of the ions depends almost exclusively on their interactions with the solvent molecules (water and CO_2), which play the role of a heat bath. This interaction then effectively thermostats the ions' temperature through collision forces without the need of introducing a Nosé–Hoover treatment explicitly to the ions.

The integration time step is set to 1 fs, ensuring good energy conservation. Each simulation is equilibrated over 10^6 to 6×10^6 time steps and 2×10^6 to 6×10^6 steps are considered for production runs, in which the thermodynamic properties of interest, such as mole fraction, molality, pressure, and density are obtained by taking the appropriate ensemble averages. The production data are also divided into 4–8 blocks, and the block averages are taken. The equilibrium time is long enough to make sure that the instant properties, such as energy and pressure, do not exhibit any drift during the production period.

The density profiles are calculated by dividing the simulation cell into 35–50 slabs in the z direction and computing the density and mole fraction in each slab. At phase coexistence conditions away from the critical locus, the system becomes inhomogeneous and naturally separates into the water-rich and CO_2-rich phases along the z direction. Note that all the calculations in this work are performed at temperatures above the critical point of CO_2, so that the system is never placed in the three-phase (liquid–liquid–vapor) region. The interfacial density profile can be fitted to an empirical hyperbolic tangent function[28]

$$\rho(z) = \frac{1}{2}(\rho_L + \rho_v) - \frac{1}{2}(\rho_L - \rho_v)\tanh\left[(z - z_0)/d\right] \tag{4}$$

where ρ_L and ρ_v correspond to the saturated liquid and vapor densities, respectively. In this equation, d represents a measure of the interfacial thickness, which is related to the "10–90" thickness parameter t, by $t = 2.1972d$.[49,50] z_0 denotes the position of the Gibbs dividing surface. Similar to density, the composition in the CO_2-rich and water-rich phases can be obtained by fitting the simulated concentration profile to Eq. 4, as shown in Figure 1.

Another important property of the vapor–liquid interface is the surface tension. This quantity can be readily evaluated using its mechanical definition involving knowledge of the diagonal elements of the pressure tensor P_{xx}, P_{yy}, and P_{zz}, through the following relation[50]

$$\gamma = \frac{L_z}{2}\left[\langle P_{zz}\rangle - 0.5 \times \left(\langle P_{xx}\rangle + \langle P_{yy}\rangle\right)\right] \tag{5}$$

where L_z is the cell length in the z direction and $\langle \ldots \rangle$ denotes canonical ensemble averages. The vapor pressure is obtained from the pressure components in the direction perpendicular to the interface, P_{zz}. The statistical uncertainty of the results is estimated by dividing the whole production period into three to four blocks of equal size and calculating the standard deviation of the block averages.

Results and Discussion

The equilibrium mole fraction of CO_2 in the water-rich (x) and CO_2-rich phases (y), the molalities m of CO_2 and NaCl in the water-rich phase (in units of moles/kg of water throughout), and the vapor–liquid interfacial tension

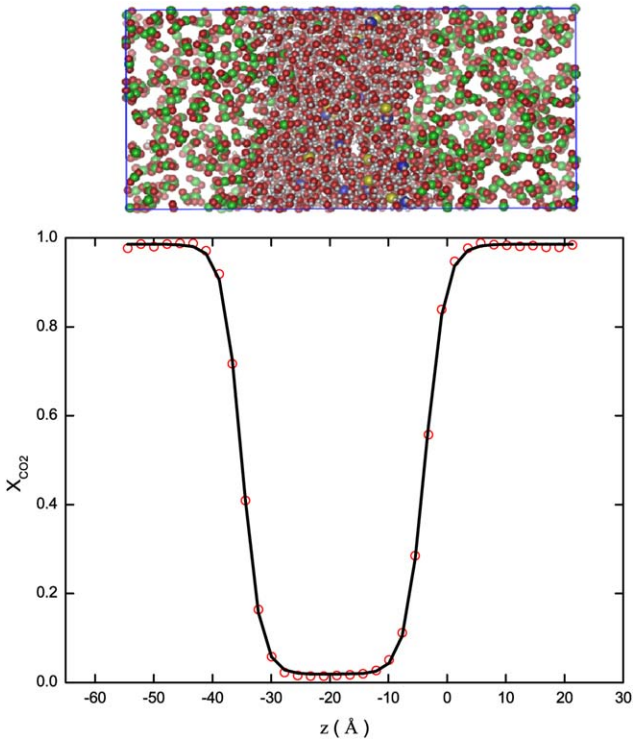

Figure 1. The concentration profile at the vapor–liquid interface using the TraPPE/TIP4P2005/SD model at 150°C, $m_{NaCl} \approx 1$.

(Top) An equilibrium configuration. Na^+ (blue), Cl^- (yellow), C (green), H (white), and O (red) atoms are shown explicitly. (Bottom) CO_2 mole fraction (open red circles) as a function of position, fitted to the hyperbolic tangent function of Eq. 4 (solid line). [Color figure can be viewed in the online issue, which is available at wileyonlinelibrary.com]

predicted by various models are listed in Tables 2–5, Supporting Information. In Figure 2, we plot the solubility of CO_2 in brine ($m_{NaCl} \approx 1$) and the corresponding composition in the CO_2-rich phase at 50°C and relatively low pressures (up to 300 bar), where experimental data are available.[51] Three combinations of CO_2-H_2O models are tested: EPM2/TIP4P2005, TraPPE/TIP4P2005, and EPM2/SPC, along with the SD model for NaCl. In our previous work,[27] the TraPPE/TIP4P2005 model was found to provide the most accurate coexistence compositions and pressures for the water-rich phase, overall. The EPM2/SPC model was found to reproduce experimental CO_2 solubility in the liquid phase at 150°C, but it overestimated this property at higher temperatures (250°C) and underestimated it at lower temperatures (50°C).[27] In this work, the molality of CO_2 in the water-rich phase and the mole fractions in the CO_2-rich phase calculated for all the models show a qualitatively correct monotonic dependence on pressure. In the water-rich phase, reasonable agreement between experimental data and simulation results is achieved using the TraPPE/TIP4P2005 model, whereas the EPM2/TIP4P2005 and the EPM2/SPC models both underpredict the CO_2 solubility by approximately 30–40%. In the CO_2-rich phase, the differences in the predicted solubility between those models become much smaller. The mole fraction of water in the vapor phase is quite small (about 0.25%), and no NaCl is found in the CO_2-rich phase.

Figure 3 shows a comparison between the pressure dependence of the interfacial tensions of the CO_2-H_2O-NaCl system predicted by the various models considered in this work, at 50°C and $m_{NaCl} \approx 1$, and the experimental values at similar conditions. All force field models predict that the interfacial tension decreases monotonically with respect to pressure. The interfacial tension predicted by the TraPPE/TIP4P2005/SD model agrees well with the data reported in Ref. 52, where a mixed salt of 0.864 (mole fraction) NaCl + 0.136 (mole fraction) KCl was used instead of NaCl. The influence of Na^+ and K^+ on the interfacial tension properties was shown to be similar by comparing results in that work with experimental data of different sources.[52] Two additional sets of experimental data from Ref. 4 are also shown in this figure. Note that at 21°C, the experimental interfacial tension shows a discontinuity due to the transition from liquid–vapor to liquid–liquid equilibrium. This discontinuity disappears at temperatures higher than the upper critical end point of CO_2–H_2O (which is almost the same as the critical temperature of pure CO_2). One would expect that the value of the surface tension at 50°C, $m_{NaCl} = 0.89$, lies between the experimental data at 21°C, $m_{NaCl} = 0.89$, and at 71°C, $m_{NaCl} = 0.89$, and that the interfacial tension at 50°C, $m_{NaCl} = 1$, would be slightly higher than at 50°C, $m_{NaCl} = 0.89$. Based on this comparison, we find that the EPM2/SPC/SD model is the most consistent with these sets of experimental data. The EPM2/TIP4P2005/SD model overestimates the interfacial tension at all pressures studied.

Figure 4 shows the mutual solubility of the CO_2-H_2O-NaCl system at 150°C over a broader range of pressure (up to 600 bar), predicted by the same combinations of models as in Figure 2. The CO_2 solubility in the water-rich phase is best predicted by the EPM2/SPC/SD model, for which the simulation results agree well with the experimental data. The TraPPE/TIP4P2005/SD model underpredicts this quantity by about 10% on average. The EPM2/TIP4P2005/SD model underestimates this quantity greatly (by roughly 30–40%), and its predictions differ increasingly from the experimental

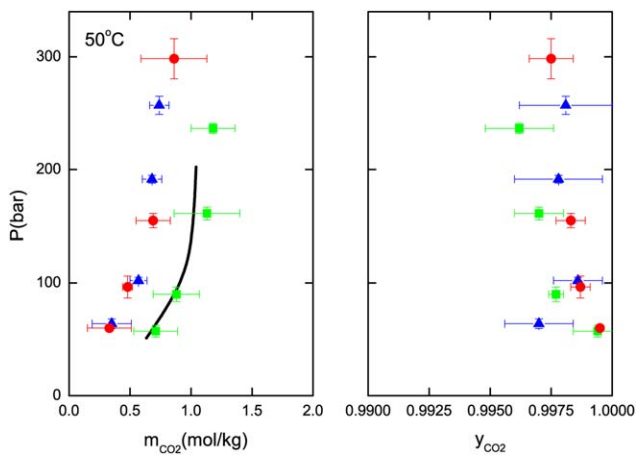

Figure 2. Solubility of CO_2 in brine (in mol CO_2/kg of H_2O) and corresponding mole fractions in the CO_2-rich phase at 50°C for $m_{NaCl} \approx 1$.

(Green square) TraPPE/TIP4P2005 model; (red circle) EPM2/TIP4P2005 model; and (blue triangle) EPM2/SPC model. SD model is used for NaCl. Experimental data of Ref. 51 are also shown (solid line). [Color figure can be viewed in the online issue, which is available at wileyonlinelibrary.com]

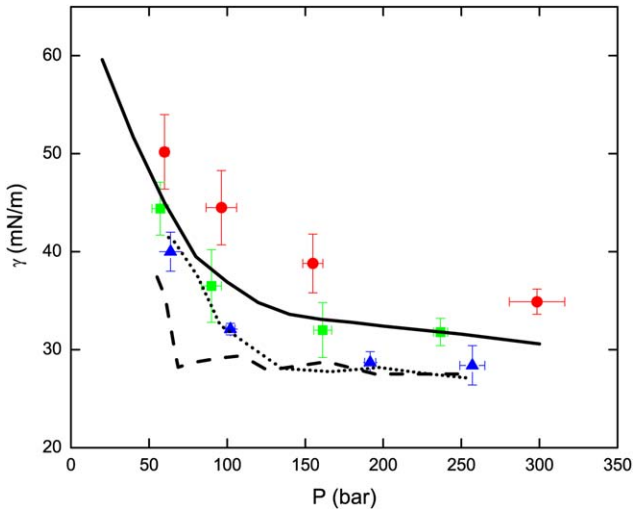

Figure 3. Interfacial tension of CO_2/H_2O/NaCl system as a function of pressure at 50°C, $m_{NaCl} \approx 1$.

Symbols for simulation results are the same as Figure 2. Experimental data of Ref. 52 for a brine composed of (0.864 NaCl + 0.136 KCl) and total salt molality = 0.98 (solid line) and experimental data of Ref. 4. $T = 71$°C, $m_{NaCl} = 0.87$ (dotted line) and $T = 27$°C, $m_{NaCl} = 0.87$ (dashed line). [Color figure can be viewed in the online issue, which is available at wileyonlinelibrary.com]

data on increasing the pressure. In the CO_2-rich phase, the EPM2/TIP4P2005/SD and TraPPE/TIP4P2005/SD models yield comparable results; the CO_2 mole fractions in the CO_2-rich phase predicted by these models are both ~2% higher than the corresponding predictions by the EPM2/SPC/SD model. Interestingly, very similar predicted trends by the three combinations of models were found in the CO_2–H_2O system (see Figures 1 and 2 in Ref. 27), with the EPM2/SPC model exhibiting the best agreement with the experimental CO_2 mole fraction in the vapor. We also point out that no NaCl is found in the vapor phase at this temperature, even at the highest pressures considered here.

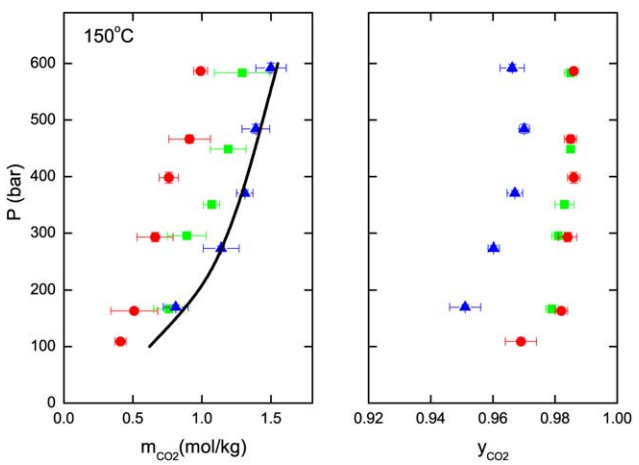

Figure 4. Solubility of CO_2 in the brine and its corresponding composition in the CO_2-rich phase at 150°C, $m_{NaCl} \approx 1$.

Symbols are the same as Figure 2. Experimental data of Ref. 54 are also shown (solid line). [Color figure can be viewed in the online issue, which is available at wileyonlinelibrary.com]

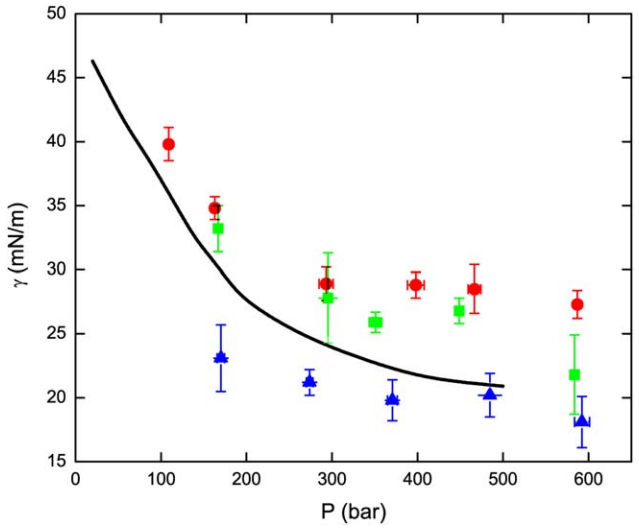

Figure 5. Interfacial tension of CO_2/H_2O/NaCl system as a function of pressure at 150°C.

Symbols for simulation and experimental results are the same as Figure 3. [Color figure can be viewed in the online issue, which is available at wileyonlinelibrary.com]

Interfacial tensions at 150°C predicted by these models are shown in Figure 5, in which we compare our simulation results with experimental values from Ref. 52. Similar to the calculations at 50°C, the interfacial tension decreases more slowly as the pressure increases and eventually approaches a plateau. Comparison with Figure 3 shows that the interfacial tension decreases with temperature, a trend that is also observed in experiments.[52] At 150°C, the TraPPE/TIP4P005/SD model overpredicts this property by ~3 mN/m on average, and the EPM2/SPC/SD model underpredicts this property by about 2 mN/m. The EPM2/TIP4P2005/SD model also yields values that are about 5 mN/m higher than the experimental data. Note that in a recent simulation study of the interfacial tension for the CO_2–H_2O system, the EPM2/

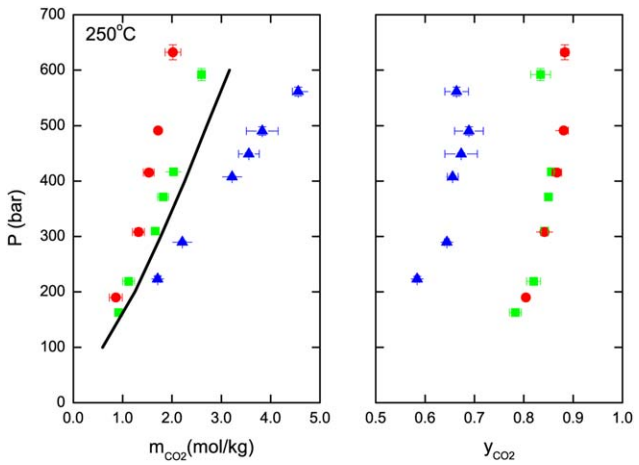

Figure 6. Solubility of CO_2 in the brine and its corresponding compositions in the CO_2-rich phase at 250°C, $m_{NaCl} \approx 1$.

Symbols are the same as Figure 2. Experimental data of Ref. 54 are also shown (solid line). [Color figure can be viewed in the online issue, which is available at wileyonlinelibrary.com]

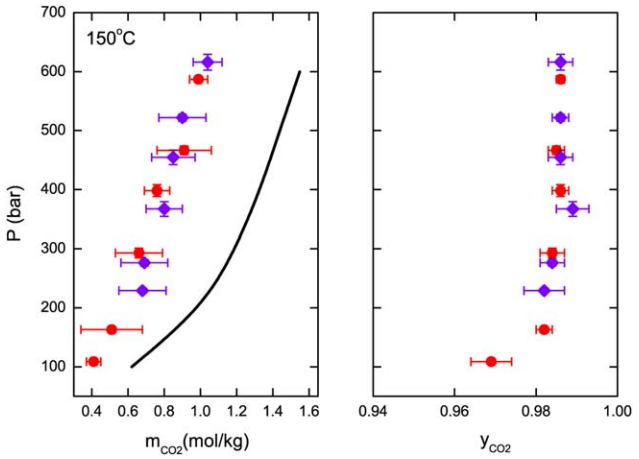

Figure 7. Solubility of CO_2 in the brine and its corresponding compositions in the CO_2-rich phase at 150°C, $m_{NaCl} \approx 1$.

(Red circle) SD model and (violet diamond) DRVH model. EPM2/TIP4P2005 model is used for CO_2/H_2O. [Color figure can be viewed in the online issue, which is available at wileyonlinelibrary.com]

TIP4P2005 model was also found to overpredict the interfacial tension relative to experimental values.[53]

Figure 6 shows the mutual solubility in the CO_2–H_2O–NaCl system at 250°C over the same range of pressures (up to 600 bar), predicted by the same combination of models as in Figure 2. At this temperature, the TraPPE/TIP4P2005/SD model is the best among the three combinations in predicting the CO_2 solubility in the liquid phase. The EPM2/TIP4P2005/SD and EPM2/SPC/SD models underpredict and overpredict the CO_2 molality, respectively, and their disagreement with the experimental data is amplified on increasing pressure. In the CO_2-rich phase, the prediction of the composition is more sensitive to the water model than to the CO_2 model, similar to the situation at 150°C. Using the

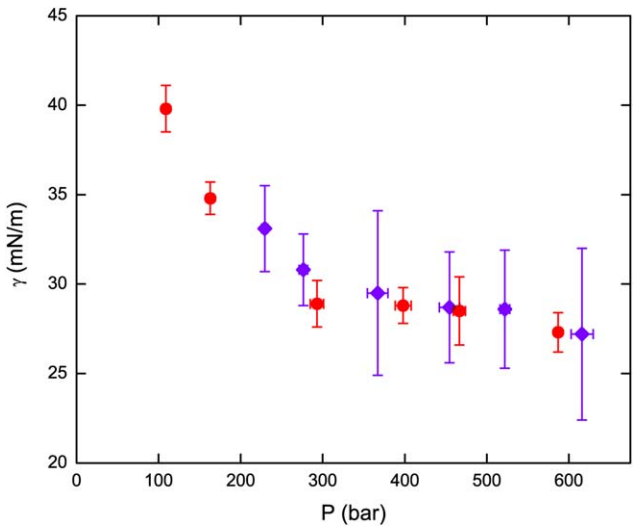

Figure 8. Interfacial tension of CO_2/H_2O/NaCl system as a function of pressure at 150°C, $m_{NaCl} \approx 1$.

Symbols are the same as Figure 7. [Color figure can be viewed in the online issue, which is available at wileyonlinelibrary.com]

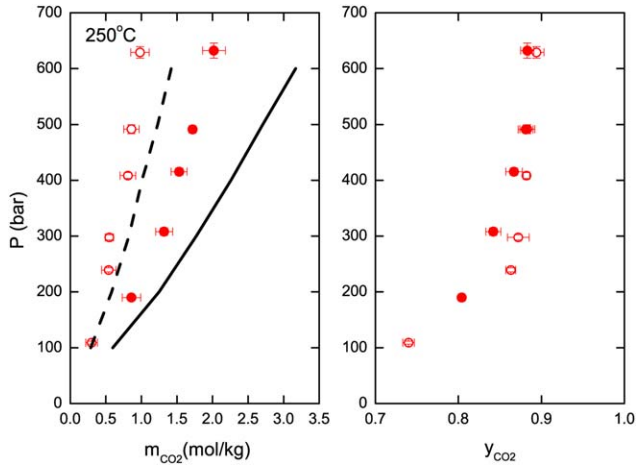

Figure 9. Solubility of CO_2 in the brine and its corresponding compositions in the CO_2-rich phase at 250°C.

(red closed circle) $m_{NaCl} \approx 1$ and (red open circle) $m_{NaCl} \approx 4$. EPM2/TIP4P2005/SD model is used for CO_2/H_2O/NaCl. Experimental data of Ref. 54 are also shown, $m_{NaCl} \approx 1$ (solid line) and $m_{NaCl} \approx 4$ (dashed line). [Color figure can be viewed in the online issue, which is available at wileyonlinelibrary.com]

same water model (TIP4P2005) but different CO_2 models (EPM2 and TraPPE), we find the simulated CO_2 mole fraction to be almost unchanged. By contrast, using the same CO_2 model (EPM2), the CO_2 mole fraction drops roughly by 25% (from ~0.8 to ~0.6) when switching from the TIP4P2005 to the SPC model. For all the models tested here, the NaCl concentration in the CO_2-rich phase is found to be zero. As the temperature increases, the system approaches its critical locus,[54] resulting in a significantly decreased surface tension compared to data at 150 and 50°C (see Tables 2–4, Supporting Information).

Comparing Figures 2, 4, and 6 to Figures 1 and 2 in Ref. 27, we find that the temperature-dependent predictive abilities of the various models studied here are very similar to the trends found in the CO_2–H_2O system, which indicates that the choice of the NaCl model may not have as big an impact as the choice of the CO_2-H_2O model in determining the phase equilibrium properties. To further evaluate the impact of the NaCl models, we adopted a newly developed NaCl model by Deublein et al.[45] (henceforth DRVH) in conjunction with the EPM2/TIP4P2005 system and compared the solubility and interfacial tension results with those of the EPM2/TIP4P2005/SD model at 150°C. The DRVH model is quite different from the SD model: its Lennard-Jones characteristic energy ε is more than three times larger. The comparisons between the two models are shown in Figures 7 and 8. As shown in Figure 7, the CO_2 solubility predicted by the two models agrees with each other within error bars in both the water-rich and CO_2-rich phases. The interfacial tensions predicted by these two models are also found to be consistent with each other, as shown in Figure 8. Despite the sharp contrast in the NaCl model parameters, our results show that for relatively low NaCl concentrations ($m_{NaCl} \approx 1$), the predictive abilities of CO_2/H_2O/NaCl models are primarily determined by the choice of CO_2/H_2O combinations and are rather insensitive to the choice of NaCl model.

As discussed in our preceding work,[27] the limited predictive ability of the various models with respect to phase

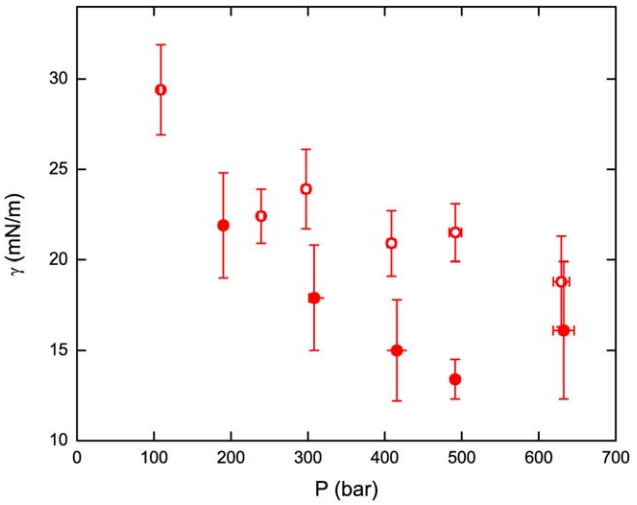

Figure 10. Interfacial tension of CO_2/H_2O/NaCl system as a function of pressure at 250°C.

Symbols are the same as Figure 9 [Color figure can be viewed in the online issue, which is available at wileyonlinelibrary.com].

equilibrium properties is largely a consequence of the inability of most water models to yield sufficiently accurate vapor pressures. As for interfacial tensions, most of the existing water models, including the SPC model, underestimate this property[55] except for the TIP4P2005 model, which is shown to reproduce the experimental surface tension of water very well.[56] The EPM2 model can also reproduce the experimental surface tension of CO_2.[57] However, when the Lorentz-Berthelot combining rules are applied, the EPM2/TIP4P2005 model overestimates the mixture's surface tensions. This effect of the Lorentz–Berthelot combining rules most likely compensates the underprediction of the SPC model and leads to the satisfactory performance of the EPM2/SPC combination at low temperatures.

In Figure 9, we evaluate the influence of salt concentration on the phase equilibrium properties of the mixtures by increasing the NaCl molality to 4 mol/kg H_2O. We conduct our investigations at 250°C using the EPM2/TIP4P2005/SD models. Upon increasing the NaCl concentration in the water-rich phase, the CO_2 solubility becomes much lower, which is commonly referred as the "salting-out" effect.[26] For the specific model studied, the discrepancies between the simulated and experimental data become smaller on increasing the NaCl concentration. The effects of salt concentration on the equilibrium properties in the CO_2-rich phase are quite small compared with that in the liquid phase. The CO_2 mole fraction increases only slightly while the NaCl concentration increases fourfold from 1 to 4 mol/kg H_2O. Once more, no salt is found in the CO_2-rich phase.

It has been shown in experiments[4,58,59] that the addition of salt leads to an increase of the interfacial tension, and there exists a linear relationship between the increase of the interfacial tension and salt concentration

$$\delta\gamma = A m_{\mathrm{NaCl}} \tag{6}$$

where $\delta\gamma$ is the increase in interfacial tension compared to the pure water system at the same temperature and pressure. The constant A is independent of temperature and pressure with a unique value of 1.43 for pressures above which the γ–P curve reaches the plateau. For pressures below which the γ–P plot reaches the plateau, the constant A fluctuates slightly and is measured to be 1.49 at 27°C, 2.53 at 71°C, and 2.22 at 100°C and is independent of pressure.[4] In Figure 10, we compare the interfacial tension for $m_{\mathrm{NaCl}} \approx 1$ and $m_{\mathrm{NaCl}} \approx 4$ at 250°C. It can be seen clearly that the addition of salt increases the interfacial tension. We also see that at this temperature, the γ–P plot does not reach the plateau before $P = 500$ bar. We then compute $\delta\gamma$ by subtracting the interfacial tension for $m_{\mathrm{NaCl}} \approx 1$ mol/kg from the interfacial tension for $m_{\mathrm{NaCl}} \approx 4$ mol/kg at each of the pressures listed in Table 3, Supporting Information below 500 bar and at $m_{\mathrm{NaCl}} \approx 1$ mol/kg, which are 109.0, 308.0, 415.6, and 491.1bar, and taking the average of the results at the four pressures. The surface tensions for $m_{\mathrm{NaCl}} \approx 4$ mol/kg at these pressures are estimated by linear interpolation between the two closest simulation data (listed in Table 3, Supporting Information) for each pressure. After dividing $\delta\gamma$ by the increase in m_{NaCl}, that is, 3 mol/kg H_2O, we found $A = 2.1$, which is within the range of the fluctuation estimated by experiments referred to earlier.

Conclusions

In this work, we investigate the phase equilibrium and surface tension properties for the vapor–liquid phase transition in the CO_2–H_2O–NaCl system, over a broad range of temperatures (50–250°C), pressures (0–600 bar), and NaCl concentrations (1–4 mol/kg H_2O) via direct interfacial MD simulations. Four combinations of models are tested: EPM2/TIP4P2005/SD, TraPPE/TIP4P2005/SD, EPM2/SPC/SD, and EPM2/TIP4P2005/DRVH.

We find that all the tested models exhibit qualitatively correct temperature and pressure dependence of CO_2 solubility in the aqueous phase. For moderate NaCl molalities (~1 mol/kg H_2O), the predictions of CO_2 solubility in the water-rich and CO_2-rich phases from the various models tested all reflect their respective predictive abilities for CO_2 solubility in pure water.[27] This shows that the predictive ability of a given model is more sensitive to the choice of the CO_2 and H_2O force fields, rather than to the NaCl model. Comparing the effects of CO_2 and water models, the latter have more impact on the prediction of vapor-phase compositions. Whether this is also the case at high NaCl concentrations deserves further investigation. Consistent with the conclusions reached in our earlier work,[27] we find that the TraPPE/TIP4P2005 model (in combination with the SD model for NaCl) is the best overall model in predicting the CO_2 solubility in the water-rich phase for temperatures below 250°C, except at 150°C, where the EPM2/SPC model outperforms the TraPPE/TIP4P2005 model.

We find that the temperature, pressure, and salt concentration dependence of the interfacial tension predicted by various models is also in agreement with experiments. The TraPPE/TIP4P2005 and EPM/SPC combinations are better in predicting the interfacial tensions at 50 and 150°C than the EPM2/TIP4P2005 model.

We demonstrate that direct interfacial MD simulations can be readily applied to determine the phase equilibrium properties of complex multicomponent fluids with reasonable accuracy. Dense multicomponent systems containing ion pairs are often difficult to study using Monte Carlo simulations incorporating unphysical moves such as insertion and deletion attempts, due to the extremely low acceptance ratio of

separating strongly interacting electrolytes. Gibbs ensemble Monte Carlo simulations applied to such systems often assume that no salt is present in the vapor phase. However, such an assumption will not hold near the critical locus where the compositions of the two phases become indistinguishable. Direct interfacial MD simulations provide a fast and simple way to check the range of applicability of Gibbs ensemble simulations. Within the range of temperature, pressure, salt concentration, and system size in our study, we find no NaCl in the CO_2-rich phase at phase coexistence.

Our work also points out the limitations of the existing models with fixed-charged, additive pair interactions in predicting phase equilibrium and interfacial properties of complex CO_2–H_2O–NaCl mixtures. We also point out that the currently widely adopted Lorentz–Berthelot combining rule is not sufficient to describe the contributions of mixing of unlike molecules to the interfacial properties. This is demonstrated by the finding that the EPM2/TIP4P2005 model overestimates the interfacial tension over the broad temperature and pressure range studied, despite the fact that the EPM2 and the TIP4P2005 model reproduce satisfactorily the CO_2 and water interfacial tension, respectively.[56,57] Further improvement of the quality of predictions using molecular simulations may result from including nonadditive corrections to the Lorentz–Berthelot mixing rule and testing the effect of polarizability and of many-body interactions. It is also worthwhile to further study the effect of the existing chemical reactions, such as $H_2O + CO_2 \leftrightarrow H_2CO_3$, on the phase behavior of the CO_2–H_2O and the CO_2–H_2O–NaCl system.

Acknowledgments

P.G.D. and A.Z.P. gratefully acknowledge the financial support of BP (Carbon Mitigation Initiative at Princeton University). A.Z.P. and P.G.D. also acknowledge support from the Department of Energy, Office of Basic Energy Sciences (grant DE-SC0002128 to A.Z.P.), and the National Science Foundation (grant CHE-0908265 to P.G.D.). Computational resources from the Terascale Infrastructure for Groundbreaking Research in Science and Engineering (TIGRESS) at Princeton University are also gratefully acknowledged.

Literature Cited

1. Metz B. Intergovernmental Panel on Climate Change, Intergovernmental Panel on Climate Change. Working Group III. Climate change 2007: Mitigation of Climate Change: Contribution of Working Group III to the Fourth Assessment Report of the IIntergovernmental Panel on Climate Change. Cambridge, New York: Cambridge University Press, 2007.
2. Schrag DP. Preparing to capture carbon. *Science*. 2007;315(5813):812–813.
3. Oldenburg CM, Lewicki JL. On leakage and seepage of CO_2 from geologic storage sites into surface water. *Environ Geol*. 2006;50(5):691–705.
4. Chalbaud C, Robin M, Lombard JM, Martin F, Egermann P, Bertin H. Interfacial tension measurements and wettability evaluation for geological CO_2 storage. *Adv Water Resour*. 2009;32(1):98–109.
5. Bachu S, Bennion DB. Interfacial tension between CO_2, freshwater, and brine in the range of pressure from (2 to 27) MPa, temperature from (20 to 125) degrees C, and water salinity from (0 to 334 000) mg L^{-1}. *J Chem Eng Data*. 2009;54(3):765–775.
6. Spycher N, Pruess K. A phase-partitioning model for CO_2-brine mixtures at elevated temperatures and pressures: application to CO_2-enhanced geothermal systems. *Transp Porous Med*. 2010;82(1):173–196.
7. Rumpf B, Nicolaisen H, Ocal C, Maurer G. Solubility of carbon-dioxide in aqueous-solutions of sodium-chloride—experimental results and correlation. *J Solution Chem*. 1994;23(3):431–448.
8. Duan ZH, Sun R. An improved model calculating CO_2 solubility in pure water and aqueous NaCl solutions from 273 to 533 K and from 0 to 2000 bar. *Chem Geol*. *14* 2003;193(3–4):257–271.
9. Ji YH, Ji XY, Feng X, Liu C, Lu LH, Lu XH. Progress in the study on the phase equilibria of the CO_2–H_2O and CO_2–H_2O–NaCl systems. *Chin J Chem Eng*. 2007;15(3):439–448.
10. Anovitz LM, Labotka TC, Blencoe JG, Horita J. Experimental determination of the activity-composition relations and phase equilibria of H_2O–CO_2–NaCl fluids at 500 degrees C, 500 bars. *Geochim Cosmochim Acta*. 2004;68(17):3557–3567.
11. Soreide I, Whitson CH. Peng-Robinson predictions for hydrocarbons, Co_2, N_2, and H_2s with pure water and Nacl brine. *Fluid Phase Equilib*. 1992;77:217–240.
12. Aranovich LY, Zakirov IV, Sretenskaya NG, Gerya TV. Ternary system H_2O–CO_2–NaCl at high T–P parameters: an empirical mixing model. *Geochem Int*. 2010;48(5):446–455.
13. Duan ZH, Moller N, Weare JH. Equation of state for the Nacl–H_2O–CO_2 system—prediction of phase-equilibria and volumetric properties. *Geochim Cosmochim Acta*. 1995;59(14):2869–2882.
14. DePaolo DJ, Orr FM. Geoscience research for our energy future. *Phys Today*. 2008;61(8):46–51.
15. Pappa GD, Perakis C, Tsimpanogiannis IN, Voutsas EC. Thermodynamic modeling of the vapor-liquid equilibrium of the CO_2/H_2O mixture. *Fluid Phase Equilib*. 2009;284(1):56–63.
16. Panagiotopoulos AZ. Direct determination of phase coexistence properties of fluids by Monte-Carlo simulation in a new ensemble. *Mol Phys*. 1987;61(4):813–826.
17. Panagiotopoulos AZ, Quirke N, Stapleton M, Tildesley DJ. Phase-equilibria by simulation in the Gibbs ensemble—alternative derivation, generalization and application to mixture and membrane equilibria. *Mol Phys*. 1988;63(4):527–545.
18. Smit B, Desmedt P, Frenkel D. Computer-simulations in the Gibbs ensemble. *Mol Phys*. 1989;68(4):931–950.
19. Ferrenberg AM, Swendsen RH. New Monte-Carlo technique for studying phase-transitions. *Phys Rev Lett*. 1988;61(23):2635–2638.
20. Ferrenberg AM, Swendsen RH. Optimized Monte-Carlo data-analysis. *Phys Rev Lett*. 1989;63(12):1195–1198.
21. Swendsen RH. Modern methods of analyzing Monte-Carlo computer-simulations. *Physica A*. 1993;194(1–4):53–62.
22. Moller D, Fischer J. Vapor–liquid-equilibrium of a pure fluid from test particle method in combination with Npt molecular-dynamics simulations. *Mol Phys*. 1990;69(3):463–473.
23. Gubbins KE. The role of computer simulation in studying fluid phase equilibria. *Mol Simul*. 1989;2(4–6):223–252.
24. LeBard DN, Levine BG, Mertmann P, Barr SA, Jusufi A, Sanders S, Klein ML, Panagiotopoulos AZ. Self-assembly of coarse-grained ionic surfactants accelerated by graphics processing units. *Soft Matter*. 2012;8(8):2385–2397.
25. Vorholz J, Harismiadis VI, Rumpf B, Panagiotopoulos AZ, Maurer G. Vapor plus liquid equilibrium of water, carbon dioxide, and the binary system, water plus carbon dioxide, from molecular simulation. *Fluid Phase Equilib*.2000;170(2):203–234.
26. Vorholz J, Harismiadis VI, Panagiotopoulos AZ, Rumpf B, Maurer G. Molecular simulation of the solubility of carbon dioxide in aqueous solutions of sodium chloride. *Fluid Phase Equilib*. 2004;226:237–250.
27. Liu Y, Panagiotopoulos AZ, Debenedetti PG. Monte Carlo simulations of high-pressure phase equilibria of CO_2–H_2O mixtures. *J Phys Chem B*. 2011;115(20):6629–6635.
28. Matsumoto M, Kataoka Y. Study on liquid vapor interface of water. 1. Simulational results of thermodynamic properties and orientational structure. *J Chem Phys*. 1988;88(5):3233–3245.
29. Trokhymchuk A, Alejandre J. Computer simulations of liquid/vapor interface in Lennard-Jones fluids: some questions and answers. *J Chem Phys*. 1999;111(18):8510–8523.
30. Rivera JL, Predota M, Chialvo AA, Cummings PT. Vapor–liquid equilibrium simulations of the SCPDP model of water. *Chem Phys Lett*. 2002;357(3–4):189–194.
31. Goujon F, Malfreyt P, Boutin A, Fuchs AH. Vapour–liquid phase equilibria of *n*-alkanes by direct Monte Carlo simulations. *Mol Simul*. 2001;27(2):99–114.
32. Rivera JL, Alejandre J. Vapor–liquid equilibrium simulations of nitrogen and *n*-alkane binary mixtures. *Colloid Surf A*. 2002;207(1–3):223–228.
33. Rivera JL, McCabe C, Cummings PT. Molecular simulations of liquid–liquid interfacial properties: water–*n*-alkane and water–

methanol–*n*-alkane systems. *Phys Rev E*. 2003;67(1). Art. No. 011603 (1–10).
34. Lopez-Lemus J, Alejandre J. Simulation of phase equilibria and interfacial properties of binary mixtures on the liquid–vapour interface using lattice sums. *Mol Phys.* 2003;101(6):743–751.
35. Inzoli I, Kjelstrup S, Bedeaux D, Simon JM. Thermodynamic properties of a liquid–vapor interface in a two-component system. *Chem Eng Sci*. 2010;65(14):4105–4116.
36. Plimpton S. Fast parallel algorithms for short-range molecular-dynamics. *J Comput Phys*. 1995;117(1):1–19.
37. Singh JK, Kofke DA. Molecular simulation study of the effect of pressure on the vapor–liquid interface of the square-well fluid. *Langmuir*. 2005;21(9):4218–4226.
38. Mecke M, Winkelmann J, Fischer J. Molecular dynamics simulation of the liquid–vapor interface: the Lennard-Jones fluid. *J Chem Phys*. 1997;107(21):9264–9270.
39. Dang LX, Chang TM. Molecular dynamics study of water clusters, liquid, and liquid–vapor interface of water with many-body potentials. *J Chem Phys.* 1997;106(19):8149–8159.
40. Pullman B. Intermolecular forces. In: Proceedings of the Fourteenth Jerusalem Symposium on Quantum Chemistry and Biochemistry held in Jerusalem, Israel, April 13–16, 1981. Dordrecht, Holland; Boston, U.S.A. Hingham, MA: D. Reidel; Sold and distributed in the U.S.A. and Canada by Kluwer Boston; 1981.
41. Abascal JLF, Vega C. A general purpose model for the condensed phases of water: TIP4P/2005. *J Chem Phys.* 2005;123(23). Art. No. 234505 (1–12).
42. Harris JG, Yung KH. Carbon dioxides liquid–vapor coexistence curve and critical properties as predicted by a simple molecular-model. *J Phys Chem.* 1995;99(31):12021–12024.
43. Potoff JJ, Siepmann JI. Vapor–liquid equilibria of mixtures containing alkanes, carbon dioxide, and nitrogen. *AIChE J*. 2001;47(7): 1676–1682.
44. Smith DE, Dang LX. Computer-simulations of Nacl association in polarizable water. *J Chem Phys.* 1994;100(5):3757–3766.
45. Deublein S, Reiser S, Vrabec J, Hasse H. A set of molecular models for alkaline-earth cations in aqueous solution. *J Phys Chem B*. 2012;116:5448–5457; Energy parameters are from private communication with Steffen Reiser, August 2012.
46. Hockney RW, Eastwood JW. Computer Simulation Using Particles, Special student ed. Bristol, England/Philadelphia: A. Hilger, 1988. Available at: http://marc.crcnetbase.com/ISBN/9781439822050. Last access date: February 12, 2013.
47. Nose S. A molecular-dynamics method for simulations in the canonical ensemble. *Mol Phys.* 1984;52(2):255–268.
48. Hoover WG. Canonical dynamics—equilibrium phase-space distributions. *Phys Rev A*. 1985;31(3):1695–1697.
49. Chapela GA, Saville G, Thompson SM, Rowlinson JS. Computer-simulation of a gas–liquid surface. 1. *J Chem Soc Faraday Trans 2*. 1977;73:1133–1144.
50. Rowlinson JS, Widom B. Molecular Theory of Capillarity. Oxford, Oxfordshire: Clarendon Press, 1982.
51. Koschel D, Coxam JY, Rodier L, Majer V. Enthalpy and solubility data of CO_2 in water and NaCl(aq) at conditions of interest for geological sequestration. *Fluid Phase Equilib*. 2006;247(1–2):107–120.
52. Li XS, Boek E, Maitland GC, Trusler JPM. Interfacial tension of (Brines + CO_2): (0.864 NaCl + 0.136 KCl) at temperatures between (298 and 448) K, pressures between (2 and 50) MPa, and total molalities of (1 to 5) mol.kg^{-1}. *J Chem Eng Data*. 2012;57(4): 1078–1088.
53. Nielsen LC, Bourg IC, Sposito G. Predicting CO_2–water interfacial tension under pressure and temperature conditions of geologic CO_2 storage. *Geochim Cosmochim Acta*. 2012;81:28–38.
54. Takenouc. S, Kennedy GC. Solubility of carbon dioxide in Nacl solutions at high temperatures and pressures. *Am J Sci*. 1965;263(5): 445–454.
55. Chen F, Smith PE. Simulated surface tensions of common water models. *J Chem Phys*. 2007;126(22). Art. No. 221101 (1–3).
56. Vega C, de Miguel E. Surface tension of the most popular models of water by using the test-area simulation method. *J Chem Phys*. 2007;126(15). Art. No. 154707 (1–10).
57. Ghoufi A, Goujon F, Lachet V, Malfreyt P. Surface tension of water and acid gases from Monte Carlo simulations. *J Chem Phys*. 2008;128(15). Art. No. 154716 (1–16).
58. Massoudi R, King AD. Effect of pressure on surface-tension of aqueous-solutions—adsorption of hydrocarbon gases, carbon-dioxide, and nitrous-oxide on aqueous-solutions of sodium-chloride and tetra-normal-butylammonium bromide at 25 degrees. *J Phys Chem-US*. 1975;79(16):1670–1675.
59. El-Maghraby RM, Pentland CH, Iglauer S, Blunt MJ. A fast method to equilibrate carbon dioxide with brine at high pressure and elevated temperature including solubility measurements. *J Supercrit Fluids*. 2012;62:55–59.

Manuscript received Sept. 18, 2012, and revision received Jan. 16, 2013.